

LASER INTERFEROMETER GRAVITATIONAL WAVE OBSERVATORY
- LIGO -
CALIFORNIA INSTITUTE OF TECHNOLOGY
MASSACHUSETTS INSTITUTE OF TECHNOLOGY

Technical Note	LIGO-T2500235-	2025/07/12
Cavity enhanced Sum Frequency Generation for indirect detection of 2 micron photons		
AMARNATH		

California Institute of Technology
LIGO Project, MS 18-34
Pasadena, CA 91125
Phone (626) 395-2129
Fax (626) 304-9834
E-mail: info@ligo.caltech.edu

Massachusetts Institute of Technology
LIGO Project, Room NW22-295
Cambridge, MA 02139
Phone (617) 253-4824
Fax (617) 253-7014
E-mail: info@ligo.mit.edu

LIGO Hanford Observatory
Route 10, Mile Marker 2
Richland, WA 99352
Phone (509) 372-8106
Fax (509) 372-8137
E-mail: info@ligo.caltech.edu

LIGO Livingston Observatory
19100 LIGO Lane
Livingston, LA 70754
Phone (225) 686-3100
Fax (225) 686-7189
E-mail: info@ligo.caltech.edu

Contents

1	Introduction	2
2	Objective	2
3	Approach	3
4	Progress	4
4.1	Complex beam parameter	5
4.2	Beam Propagation	6
4.3	Mode matching to the Cavity	7
4.4	Bow-tie Cavity Scan	8
4.4.1	Cavity Resonance Condition	8
4.4.2	Laser Frequency Scanning via Thermal Tuning	9
4.4.3	Transmission Scan and Mode Matching estimate	9
5	Timeline	11
6	detailed plan for rest of the summer	11

1 Introduction

The current generation Laser Interferometer Gravitational Wave Observatory (LIGO) uses the 1064 nm Nd:YAG lasers for precise measurements of the strain of order of 10^{-21} in its 4-km long arms . This wavelength was chosen because of several reasons including the well-established performance of 1064 nm neodymium-doped yttrium aluminum garnet (Nd:YAG) laser systems, narrow linewidth and availability of excellent frequency and power stabilization techniques. Additionally, fused silica, the material used for LIGO's test masses exhibits minimal absorption at this wavelength. Further the detection is also favoured because of the availability of high quantum efficiency Photodetectors (PD) at 1064 nm. The next generation LIGO aims to further increase the sensitivity, one way to do so is by reducing the thermal noise [1] which is a major source of noise at frequencies ranging from 40 Hz to few hundred Hz. Interestingly, Crystalline silicon when cryogenically cooled offers low absorption and thermal noise at longer wavelengths around 2 micron. Hence this shift of material along with laser wavelength is expected to increase the sensitivity of the detector.

However, One of the challenges in using a 2-micron laser is the low quantum efficiency PD available at 2 microns, causing less photon detection thus signal loss. Hence, the goal is to convert the 2-micron photons to a shorter wavelength of 700 nm where the available silicon PD have excellent quantum efficiency. This motivates the usage of the Sum Frequency Generation (SFG) for indirect detection of 2 micron photons. SFG is a 2nd order non-linear optical process where two input photons at angular frequency ω_1 and ω_2 are overlapped in a non-linear crystal resulting in photons of angular frequency $\omega_3 = \omega_1 + \omega_2$ having energy equal to simple addition of energies of the both the input photons. The 2 micron light is combined with 1064 nm pump beam in periodically poled lithium niobate (PPLN) crystal resulting in the generation of visible 700 nm photons, which can be detected by the available high quantum efficiency silicon PD thus enabling an indirect detection of the 2-micron light.

Initial single pass experiments where the pump beam passes through the PPLN crystal only once have demonstrated the feasibility of converting 2 micron photons to 700 nm. However the measured up-conversion efficiency was much lower than the theoretical predictions. The reported reason for this consistently lower efficiency is mainly due to low pump power of around 2 mW. Additionally there was poor spatial mode overlap of the pump and signal photons which along with non uniform poling and defects in the PPLN crystal, coating absorption and transmission losses affects the overall efficiency of the SFG. This work will focus on cavity-enhanced SFG to improve the conversion efficiency. In this method the PPLN crystal will be placed inside an optical cavity resonant to the pump of 1064 nm. This resonant optical cavity will cause the pump light to circulate multiple times within the cavity causing build up of higher pump power and increased optical path length across the PPLN crystal thus increased non-linear interaction and increased efficiency of the up conversion of 2 micron to 700 nm.

2 Objective

The focus of this work is to setup and characterize a cavity-enhanced sum-frequency generation system for the efficient upconversion of 2 micron photons to 700 nm thus eventually

having indirect detection of the 2 micron photons. This will include setting up the optical cavity, mode matching, proper spatial mode overlap of the pump and signal beam, optimization of the overlap parameters, investigating thermal lensing in the high power cavity and damage thresholds for the optics used. Further we have to check the losses due to the defects in the PPLN crystal. Finally we have to investigate the various noise from laser power, polarization, frequency and other sources which are coupling in the cavity.

3 Approach

The initial stage will consist of setting up and alignment of the bow tie cavity and experimental apparatus. Since every optical cavity has a mode associated with it, we need to align the laser using lenses such that the mode of the laser beam matches the mode supported by the cavity at the Input of the cavity. After proper mode matching, the PPLN crystal and oven can be introduced inside the cavity and cavity alignment can be done. Once the cavity is aligned with crystal in place then Pound-Drever-Hall (PDH) locking of the cavity is required to lock the cavity to the fundamental mode. The pump beam at 1064 nm and the signal beam at 2 μm will be aligned on the optical table using precision mounts and optics. After stable experimental operation experiments will be conducted and the data will be taken to analyze the up-conversion efficiency. Parametric dependence of the upconversion efficiency can be studied in the end.

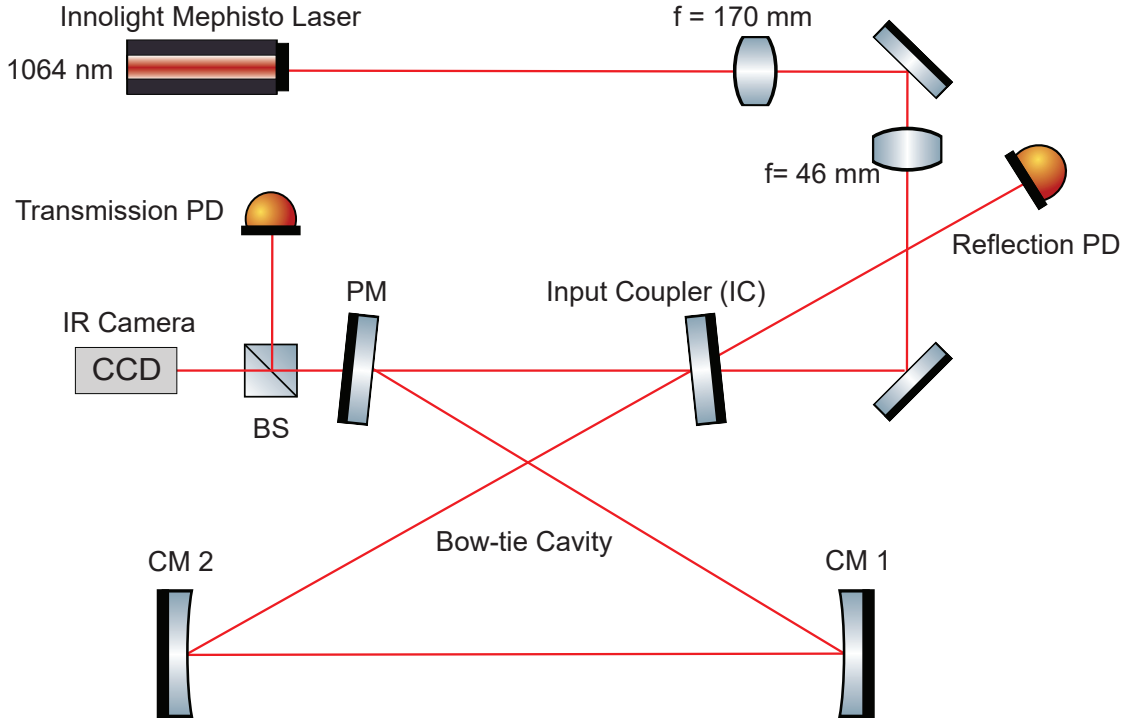


Figure 1: pump resonant cavity schematic.

4 Progress

Figure 1 Shows a simplified schematic of the 1064 nm pump resonant cavity. Table 1 shows the specifications of the cavity mirrors. An innolight mephisto 1064 nm laser propagates through a pair of mode-matching lenses to the plane mirror Input Coupler (IC) of the cavity. The beam undergoes transmission through the IC then it gets reflected from the plane mirror (PM) to the curved mirror (CM1) from where it goes to curved mirror (CM2) then finally back to IC and the propagation repeats. A small leakage through the PM is fed to beam splitter (BS) which sends the transmission to an IR camera and a transmission PD. A part of the input beam is reflected from the IC and a part of the beam leaks from inside of the cavity both of these are collected by the reflection PD.

Mirror	Type	RoC [m]	T	R
IC	Flat	∞	0.003	—
PM	Flat	∞	—	0.999
CM1	Curved	0.2	—	0.999
CM2	Curved	0.2	—	0.999

Table 1: Mirror Specifications for Bow-tie Cavity

Alignment is very important in such an experiment where the efficiency of the upconversion depends on spatial mode overlap, mode matching, etc. The SFG setup was aligned using a pair of Irises to make sure that the laser (1064 nm) is propagating at the same level everywhere. The aligned experimental setup can be seen in the figure 2.

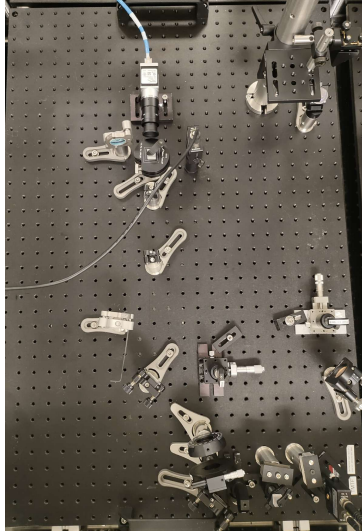


Figure 2: Aligned Experimental setup for cavity-enhanced sum-frequency generation.

An optical cavity supports several Electromagnetic modes which can resonate inside it. The fundamental mode is the gaussian or TEM00 mode which is spherical spot with gaussian intensity distribution. there exists other higher order modes which have different intensity distributions, some of the higher order modes of an optical cavity are shown in the figure 3. For higher upconversion efficiency we require good spatial mode overlap between the pump

and 2 micron thus the fundamental mode is desired. Mode matching is required such that most of the power is coupled into the fundamental mode and less power is higher order modes.

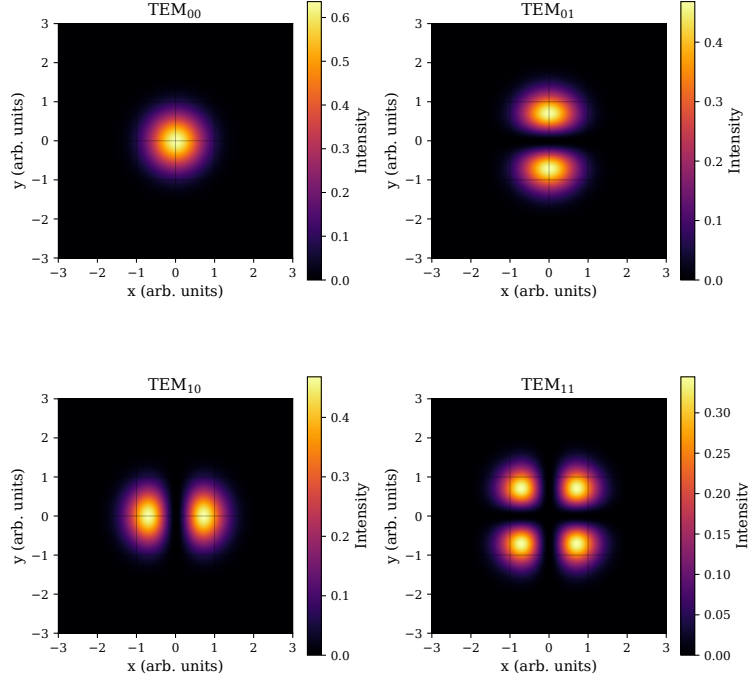


Figure 3: some higher order modes supported by an optical cavity.

4.1 Complex beam parameter

Any gaussian laser beam propagating along z direction can be associated with a complex parameter or q parameter at any position z . The complex beam parameter $q(z)$ at position z is defined as:

$$q(z) = (z - z_0) + iZ_R \quad (1)$$

where:

- z is the axial distance along the beam propagation direction.
- z_0 is the location of the beam waist (position where the beam radius is minimum).
- Z_R is the Rayleigh range, given by:

$$Z_R = \frac{\pi w_0^2}{\lambda} \quad (2)$$

- w_0 is the beam waist (minimum width) which is situated at z_0 .

- λ is the laser wavelength.

This q parameter $q(z)$ is sufficient to get all the information about the beam such as the $1/e^2$ width $w(z)$ and radius of curvature $R(z)$.

$$\frac{1}{q(z)} = \frac{1}{R(z)} - i \frac{\lambda}{\pi w^2(z)} \quad (3)$$

where:

- $R(z)$ is the radius of curvature of the phasefront at position z .
- $w(z)$ is the beam width at position z .

This q parameter formulation can be utilized for the mode matching purpose.

4.2 Beam Propagation

Given a gaussian beam defined at some position with some initial q parameter q_0 . This beam can be propagated through a system consisting of a combination of free space, lenses or other optical componensts using ray transfer matrices or ABCD matrices to get the output q parameters.

- **Free Space Propagation (distance L):**

$$M_{\text{free space}} = \begin{bmatrix} 1 & L \\ 0 & 1 \end{bmatrix} \quad (4)$$

- **Thin Lens (focal length f):**

$$M_{\text{lens}} = \begin{bmatrix} 1 & 0 \\ -\frac{1}{f} & 1 \end{bmatrix} \quad (5)$$

For a system involving N elements with individual matrices M_1, M_2, \dots, M_N , the complex system can be replaced by a single matrix which is the product of all the matrices in the sequence as:

$$M_{\text{total}} = M_N \times M_{N-1} \times \dots \times M_2 \times M_1 = \begin{bmatrix} A & B \\ C & D \end{bmatrix} \quad (6)$$

where A , B , C , and D are the elements of the matrix obtained after all the matrix multiplications.

The complex beam parameter after propagation through complex system is expressed using the ABCD law:

$$q_{\text{out}} = \frac{Aq_{\text{in}} + B}{Cq_{\text{in}} + D} \quad (7)$$

4.3 Mode matching to the Cavity

Proper spatial mode overlap is desired for higher efficiency of the SFG. thus it is required that the laser beam incident at the input coupler must have nearly equal beam width and curvature as supported inside the cavity. Any mode mismatch causes power to couple into higher modes which are not desired. This can be equivalently be stated that we want the cavity q parameter at IC to be equal to the propagating beam's q parameter at IC which ensures the beam width and radius of curvatures both to be matched.

The primary task for this experiment was to check the mode matching status that is the mode of the laser beam coming incident to the Input coupler (Here, first plane mirror of the cavity) should match to the mode supported to the cavity. Mode matching was checked by taking the beam profile using a scanning slit beam profiler to measure beam widths along both x and y directions and the data was fitted to the following gaussian beam propagation equation:

$$w(z) = w_0 \sqrt{1 + \left(\frac{z - z_0}{z_R} \right)^2}, \quad z_R = \frac{\pi w_0^2}{\lambda} \quad (8)$$

Waist and its position uniquely determines the q parameters, which can then be propagated via ABCD matrices for a pair of lenses and free spaces to obtain the q at the IC. Lens positions and focal lengths can be adjusted to obtain a solution which matches with the mode supported by the cavity. finally the lenses were placed and the resultant mode near the IC matches the mode supported by the cavity as shown in the figure 4.

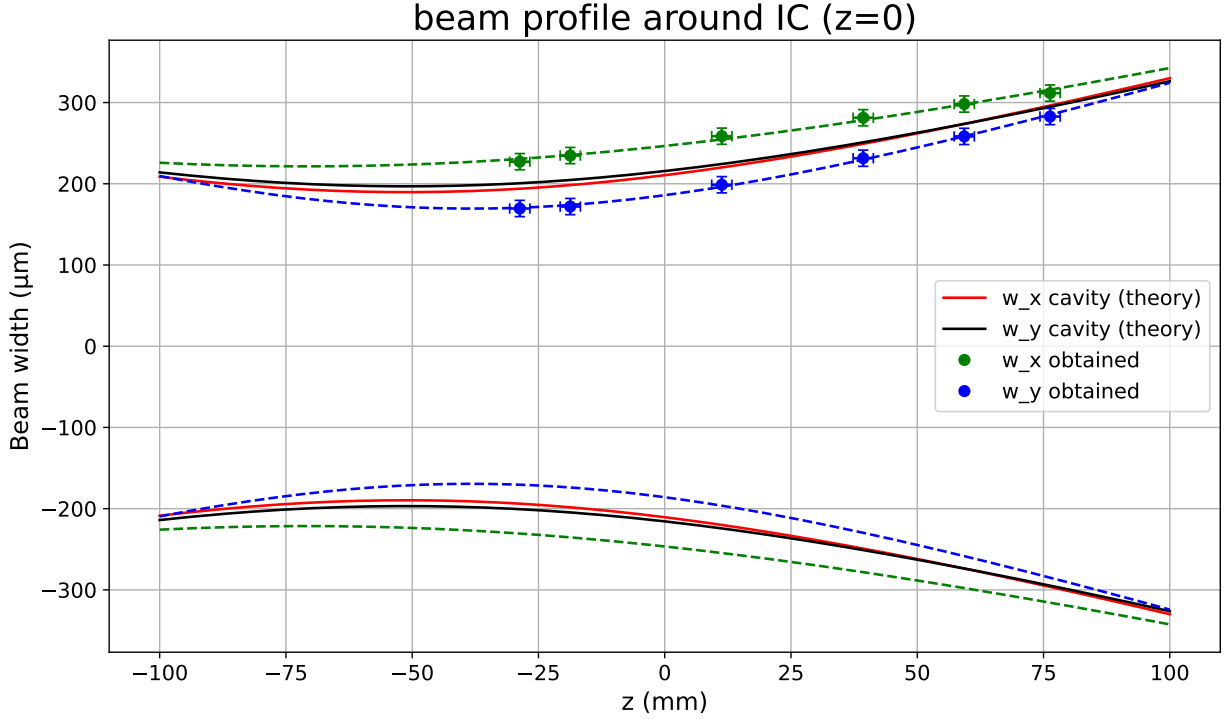


Figure 4: Beam profile measurements fitted to the gaussian beam propagation.

This fitting provided estimates for the beam waist w_0 and waist location z_0 thus uniquely

giving q parameter. The beam profile measurements are fitted using the above equation. figure 4 shows that the experimentally obtained resulatnt mode is close to the theoretical simulation mode obtained from finesse. It should be noted the the lens positions can be adjusted within a few millimeters for tuning the mode, thus all the lenses were mounted on a translation stage.

4.4 Bow-tie Cavity Scan

The bow-tie cavity shown in the figure 1 was aligned by the following procedure: The IC was removed and using the steering mirrors the beam was aligned to the center of the PM, then the PM was adjusted to get the beam on the center of CM1 which was then used to align the beam to center of CM2 and finally CM2 was used to align the outgoing beam from the cavity to spatially overlap the incoming beam at the position of the IC, this can be done using a beam viewer card with two holes on it. The outgoing beam was referenced to an Iris (pinhole) far away. Finally the IC was placed back and oriented such that the reflection from it aligned to the reference Iris.

4.4.1 Cavity Resonance Condition

There is a need to characterize and align an optical cavity before proceeding to PDH locking of the cavity. It is necessary to scan the cavity either by changing the cavity length using a PZT or by changing the laser frequency and observe transmission and reflection signals to identify resonance peaks and coupled energy in different modes.

A **bow-tie** optical cavity resonates[2] when the round-trip phase condition is satisfied:

$$L = m\lambda, \quad m \in \mathbb{Z} \quad (9)$$

where:

- L is the **round-trip length** of the cavity, λ is the laser wavelength and m is an integer.

Equivalently, the resonance condition can be expressed in terms of the separation between adjacent resonances which is known as the Free Spectral Range (FSR) and for a **bow-tie cavity** it is defined as:

$$\text{FSR} = \frac{c}{L} \quad (10)$$

where:

- c is the speed of light in vacuum,
- L is the **round-trip length** of the cavity.

In this experiment, the round-trip length of the bow-tie cavity is approximately $L = 0.8 \text{ m}$. Substituting this into the FSR formula:

$$\text{FSR} = \frac{3 \times 10^8 \text{ m/s}}{0.8 \text{ m}} = 375 \text{ MHz} \quad (11)$$

To scan atleast one full cavity resonance, the laser frequency/cavity length must be swept over to cover at least one FSR value, i.e., approximately 375 MHz in this case.

4.4.2 Laser Frequency Scanning via Thermal Tuning

The Innolight Mephisto NPRO laser used in this setup allows frequency tuning by adjusting the temperature of the monolithic crystal inside, by using a modulation input. This tuning mechanism enables slow but wide-range frequency sweeps suitable for cavity scanning. The relationship between laser frequency ν and temperature T is approximately linear over small ranges:

$$\frac{d\nu}{dT} \approx 3 \text{ GHz/K}, \quad \frac{dT}{dV} \approx 1 \text{ K/V} \quad \Rightarrow \quad \frac{d\nu}{dV} \approx 3 \text{ GHz/V} \quad (12)$$

Thus, applying a small triangle or ramp voltage 125 mV_{pp} (peak to peak) to the temperature modulation port results in a frequency sweep of:

$$\Delta\nu = (3 \text{ GHz/V}) \times 0.125 \text{ V} = 375 \text{ MHz} \quad (13)$$

This is sufficient to scan across approximately 1 free spectral ranges (FSRs) of the cavity. It is important to note that the Mephisto laser also supports high-speed frequency tuning

via an internal piezoelectric transducer (PZT), but the PZT tuning range is limited to approximately $\pm 100 \text{ MHz}$. Therefore, for scanning atleast one FSR in this experiment, thermal tuning is preferred.

4.4.3 Transmission Scan and Mode Matching estimate

Cavity was scanned using a function generator to get 150 mV_{pp} Ramp signal with frequency of 20 MHz (50 seconds time period). The output of the function generator was connected to temperature controller's modulation port.

Measurement of Mode Matching Efficiency:

The transmission photodiode (PD) signal was recorded over a time duration approximately spanning a FSR of the cavity. The largest transmission peak in the scan was identified as the TEM_{00} mode, as confirmed by using an IR camera to the spatial mode profile simultaneously during data acquisition. The mode matching efficiency was estimated using the ratio of the background-subtracted peak heights of the TEM_{00} mode to the total power coupled into all visible transverse modes:

$$\eta = \frac{\sum(V_{\text{TEM}_{00}} - V_{\text{offset}})}{\sum(V_{\text{TEM}_{00}} - V_{\text{offset}}) + \sum(V_{\text{HOM}} - V_{\text{offset}})} \quad (14)$$

where:

- $V_{\text{TEM}_{00}}$ is the peak voltage corresponding to the fundamental mode,
- V_{HOM} are the peak voltages of the higher-order modes (HOMs),
- $V_{\text{offset}} = 53 \text{ mV}$ is the measured background offset voltage of the photodetector.

Using this method, the estimated mode matching efficiency was found to be approximately:

$$\eta \approx 0.58 \quad \text{or} \quad 58\%$$

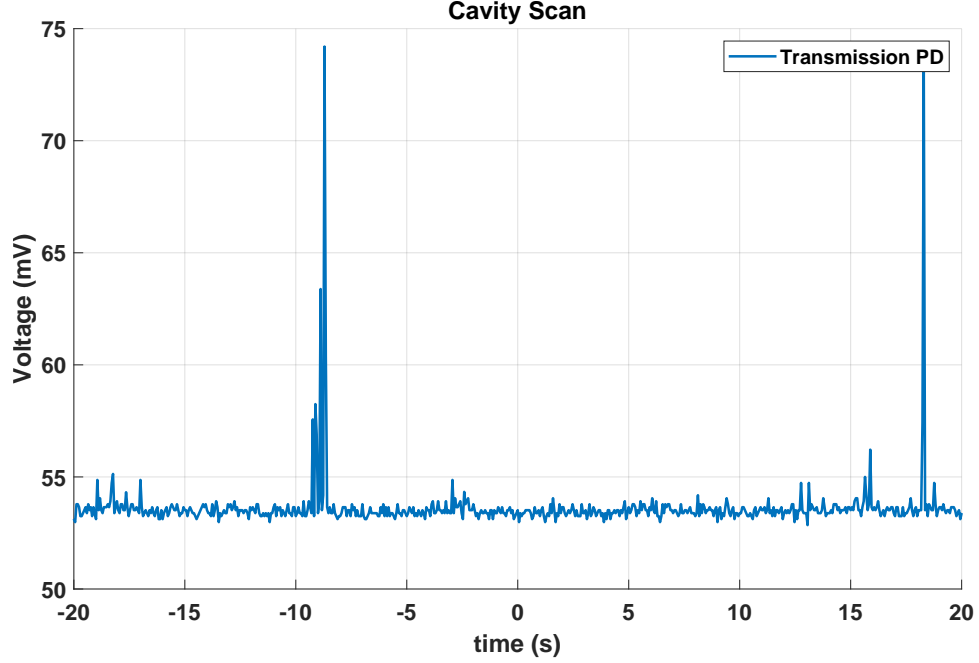


Figure 5: Cavity scan by thermal tuning

This indicates that more than half of the incident photons are successfully coupled into the TEM_{00} mode of the cavity.

It was further observed that the mode matching efficiency is highly sensitive to the precise positioning of the mode-matching lenses, which were mounted on a translation stage. Small changes (on the order of millimeters) in lens separation significantly affected the observed TEM_{00} peak height and the appearance of higher-order modes.

5 Timeline

Week 1 : Intoduction to lab, techniques of cavity design, Study earlier version experiments.

Week 2 : Setting up components on optical table and alignment as per the experimental design.

Week 3 : Mode matching calculations

Week 4 :Implementing different mode matching solutions

Week 5 : Setting up the Cavity alignment

Week 6 : Cavity sweep and mode matching measurements

Week 7 : Setting up PPLN oven

Week 8 : PDH locking the cavity and Aligning 2 um laser

week 9 : SFG upconversion measurements

Week 10 : More measurements and report writing and final presentation.

6 detailed plan for rest of the summer

Aligning the bow tie cavity for flashing and setting up the moku lab for data collection. planning and implementation of the laser frequency scanning using PZT or thermal tuning.

Setting up the Oven for the PPLN: PPLN oven mount has to be setup inside the bow-tie cavity at halfway as per the finesse model. We need to set up the PID controls for temperature adjustments.

PDH locking: Obtaining the PDH error signal and locking the cavity to the fundamental mode.

Aligning 1064 nm pump and 2 μm sources working on spatial mode overlap : The 1064 nm pump needs to be spatially aligned with the 2 micron light inside the cavity. first task is to learn the protocols for operating the 2 micron laser then it will be aligned inside the cavity. for maximum up conversion efficiency mode lap integral will be used to set the waist of the 2 micron light.

Running the SFG experiment and Taking measurement of the up conversion efficiency : experimental data will be taken and analyzed to get the up conversion (to 700 nm) efficiency. This will be done by varying the pump power (can be achieved using polarizer).

Studying the dependence of parameters such as polarization, power, crystal temperature, etc. measurements will be taken by introducing systematic variations of polarization, power, crystal emperature to study the dependence of these. Taking Up conversion measurements and analyzing the data Experimental data will be analyzed and the measured efficiency including potential losses will be plotted against the theoretical predictions then finally drawing conclusions, preparing the work repot and presentation.

References

- [1] G.M. Harry, A.M. Gretarsson, P.R. Saulson, et al., “Thermal noise in interferometric gravitational wave detectors due to dielectric optical coatings,”
- [2] P. Patimisco, A. Sampaolo, F.K. Tittel, V. Spagnolo, “Mode matching of a laser-beam to a compact high finesse bow-tie optical cavity for quartz enhanced photoacoustic gas sensing,” *Sensors and Actuators B: Chemical*, vol. 259, pp. 828–833, 2018.